Hindawi Publishing Corporation
EURASIP Journal on Wireless Communications and Networking
Volume 2009, Article ID 406028, 10 pages
doi:10.1155/2009/406028

Research Article

Diversity Techniques for Single-Carrier Packet Retransmissions over Frequency-Selective Channels

Abdel-Nasser Assimi, Charly Poulliat, and Inbar Fijalkow (EURASIP Member)

ETIS, CNRS, ENSEA, Cergy-Pontoise University, 6 avenue du Ponceau, 95000 Cergy-Pontoise, France

Correspondence should be addressed to Abdel-Nasser Assimi, abdelnasser.assimi@ensea.fr

Received 16 February 2009; Revised 16 June 2009; Accepted 16 August 2009

Recommended by Stefania Sesia

In data packet communication systems over multipath frequency-selective channels, hybrid automatic repeat request (HARQ) protocols are usually used in order to ensure data reliability. For single-carrier packet transmission in slow fading environment, an identical retransmission of the same packet, due to a decoding failure, does not fully exploit the available time diversity in retransmission-based HARQ protocols. In this paper, we compare two transmit diversity techniques, namely, cyclic frequency-shift diversity and bit-interleaving diversity. Both techniques can be integrated in the HARQ scheme in order to improve the performance of the joint detector. Their performance in terms of pairwise error probability is investigated using maximum likelihood detection and decoding. The impact of the channel memory and the modulation order on the performance gain is emphasized. In practice, we use low complexity linear filter-based equalization which can be efficiently implemented in the frequency domain. The use of iterative equalization and decoding is also considered. The performance gain in terms of frame error rate and data throughput is evaluated by numerical simulations.

1. Introduction

Single carrier with cyclic-prefix transmissions has recently gained a certain attention, especially after its adoption for the uplink in the 3GPP Long-Term-Evolution (LTE) standard [1]. Actually, single-carrier signaling provides a low peak-to-average power ratio (PAPR) compared to the orthogonal frequency division multiplexing (OFDM). Moreover, the insertion of a cyclic prefix allows simplified signal processing in the frequency domain at the receiver. Reliable data communication systems usually implement HARQ protocols [2] in order to combat errors introduced by the communication channel. This includes channel noise and intersymbol interference (ISI) resulting from multipath propagation in wireless channels. In order to reduce the effect of the ISI on the performance of the system, one could implement a sophisticated detection scheme at the receiver, such as a turboequalizer [3], for example, at the expense of increased receiver complexity. Another possibility is to use a simple linear equalizer with a low rate channel code in order to handle the residual interference remaining after equalization. The price to pay for this solution is reduced data throughput, even in good channel conditions.

In the context of HARQ protocols, joint equalization of multiple received copies of the same packet significantly enhances system performance, especially when there is channel diversity among subsequent HARQ transmissions. When a part of the available bandwidth falls in a deep fading, a decoding failure may occur and a retransmission request is made by the receiver. An identical retransmission of the same packet would suffer from the same problem if the channel remains unchanged. Combining both received packets provides some signal-to-noise ratio (SNR) gain resulting from noise averaging, but the interference power remains the same.

In order to enhance the joint detection performance, many transmit diversity schemes have been proposed for multiple HARQ transmissions. When channel state information at the transmitter (CSIT) is available, precoding (preequalization) techniques [4, 5] can be used at the transmitter in order to transform the frequency selective channel into a flat channel. In [6], linear precoding filters

are optimized for multiple HARQ transmissions. In general, linear filtering increases the PAPR of the transmitted signal, especially when the channel response contains a deep fading. Note that methods based on the availability of CSIT require an increased load on the feedback channel. In addition, these methods can be sensitive to channel mismatch and can not be applied when the channel changes rapidly from one transmission to the next.

For communication systems with very limited feedback channels, the CSIT assumption is not applicable. However, in the absence of CSIT, there are some useful techniques that enhance the system performance in slow time-varying channel conditions while keeping the system performance unchanged in fast changing channel conditions without the need for switching mechanisms. In the absence of CSIT, a phase-precoding scheme has been proposed in [7]. In this scheme, a periodic phase rotation pattern is applied for each HARQ transmission in order to decorrelate the ISI among the received copies of the same packet. This can be seen in the frequency domain as a frequency shift by more than the coherence bandwidth of the channel. The advantage of the phase-precoding transmit diversity scheme is the conservation of the power characteristics of the transmitted symbols. Hence, it does not increase the PAPR of the transmitted signal. Another transmit diversity scheme is the bit-interleaving diversity initially proposed in [8] for noncoded transmissions using iterative equalization at the receiver. This scheme outperforms joint equalization of identically interleaved transmissions but it has higher complexity. For coded transmissions, it has been found in [9] that the iterative equalization approach is not suitable for the bit-interleaving diversity. Performing separate equalization with joint decoding instead leads to a significant performance improvement and reduced complexity. In [10], a mapping diversity scheme was proposed for high-order modulations. This scheme results in an increased Euclidean distance separation between transmitted frames. The drawback of this method is to be limited to high-order modulations which makes it not applicable for BPSK or QPSK modulations.

In this paper, we compare two transmit diversity schemes: the cyclic frequency-shift diversity and the bit-interleaving diversity. The theoretical comparison is performed assuming optimal ML detection and decoding. Since the ML receiver is practically nonrealistic, an iterative receiver using a turboequalizer is considered in this paper in order to verify the theoretical results. However, the performance of a noniterative receiver is also evaluated for low complexity requirements.

The remaining of this paper is organized as follows. In Section 2, the system model for both diversity schemes is introduced. In Section 3, we investigate their respective performance using an optimal ML receiver. In Section 4, we present the corresponding receivers and investigate their respective complexity. In Section 5, we give some simulation results showing the advantages of each diversity scheme for different system parameters. Finally, conclusions are given in Section 6.

Notation. The following notations are used throughout this paper. Uppercase boldface letters ($\mathbf{A}$) denote matrices; lowercase boldface letters ($\mathbf{a}$) denote (column) vectors, and italics (a, A) denote scalars; an ensemble of elements is represented with calligraphic fonts ($\mathcal{A}$).

2. System Model

We consider the communication system model shown in Figure 1 using single carrier bit-interleaved coded modulation with multiple HARQ transmissions over a frequency selective channel.

A data packet $\mathbf{d}$, of KQ information bits including cyclic redundancy check (CRC) bits for error detection, is first encoded by a rate-K/N error correction code to obtain QN coded bits $\mathbf{c}$. The codeword $\mathbf{c}$ is stored at the transmitter in order to be retransmitted later if it is requested by the receiver due to a transmission error. Each branch in Figure 1 corresponds to a single transmission of the same packet. Thus, for $t = 1, 2, \ldots, T$, the tth branch corresponds to the tth (re)transmission of $\mathbf{c}$ according to the considered HARQ scheme.

For the first transmission of the coded packet, a bit-interleaver $\pi^{(1)}$ is applied on $\mathbf{c}$ in order to statistically decorrelate the encoded bits. The obtained coded and interleaved bits $\mathbf{c}^{(1)}$ are then mapped into a sequence of N symbols, denoted by $\mathbf{s}^{(1)}$, using a complex constellation alphabet $\mathcal{S}$ of size $|\mathcal{S}| = 2^Q$ symbols having unit average power. The modulated symbols are then processed by a channel precoder to generate the signal $\mathbf{x}^{(1)}$. In this paper, the channel precoder performs a simple cyclic frequency-shift (CFS) operation on the signal $\mathbf{s}^{(1)}$. Before the transmission of $\mathbf{x}^{(1)}$ over the propagation channel, a cyclic prefix (CP) of length P is inserted at the beginning of the packet in order to avoid interpacket interference and to facilitate the equalization in the frequency domain.

At the receiver side, if the packet is successfully decoded by the receiver, a positive acknowledgment (ACK) signal is returned to the transmitter through an error-free feedback channel with zero delay; otherwise a negative acknowledgment (NACK) signal is returned indicating a decoding failure. In the latter case, the transmitter responds by resending the same coded packet $\mathbf{c}$ but in a different way according to the considered transmit diversity scheme. If the packet is still in error after a maximum number $T_{\max}$ of allowable transmissions (the first transmission plus $T_{\max} - 1$ possible retransmissions), an error is declared and the packet is dropped out from the transmission buffer.

Note that this model corresponds to SC-FDMA transmission in LTE system when each user is allocated the entire system bandwidth as in time division multiplexing. However, the main results of this paper are still applicable when the same subcarriers are allocated to the user during all HARQ retransmissions by considering the equivalent channel response seen by the user's carriers. We define three transmission schemes.

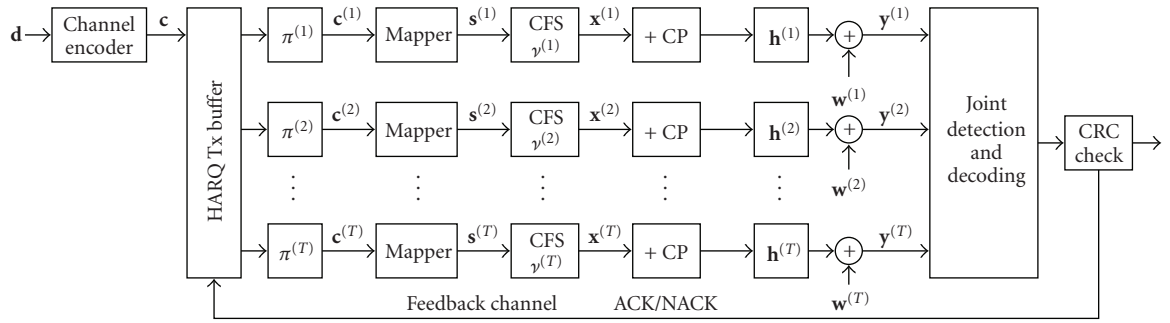

Figure 1: System model for single-carrier cyclic-prefix transmit diversity for HARQ retransmission protocols.

(a) Identical Transmissions (IT) Scheme. In this scheme, the same interleaver is used for all transmissions with no channel precoding. As stated in the introduction of this paper, the benefit of the IT-HARQ scheme in slow time-varying channels is the SNR gain due to noise averaging. This scheme is used as a reference in order to evaluate the gain introduced by the other diversity schemes.

(b) Bit-interleaving Diversity (BID) Scheme. In this scheme, a different bit-interleaver is used for each retransmission with no channel precoding.

(c) Cyclic Frequency-Shift Diversity (CFSD) Scheme. In this scheme, the same interleaver is used for all transmissions but a different channel precoder is used for each transmission. The precoder cyclically shifts the transmitted signal in the frequency domain by the normalized frequency value $\nu^{(t)} = k/N$ for $k \in [0, N-1]$, where t denotes the HARQ transmission index. This operation can be performed in the time domain by

$$x^{(t)}(n) = e^{j2\pi n\nu^{(t)}} s^{(t)}(n), \tag{1}$$

for $n = 0, \ldots, N-1$.

The transmission channel is frequency-selective modeled by its equivalent complex-valued discrete-time finite impulse response of length L, denoted by $\mathbf{h}^{(t)} = (h^{(t)}(0), \ldots, h^{(t)}(L-1))$ assumed constant during the period of one packet transmission. Each channel tap is a zero mean complex random variable with a given variance which is determined from the power-delay profile of the channel. In addition, we assume that the channel response changes slowly from one transmission to the next. In our analysis, we consider the long-term static channel model where the channel remains the same for all HARQ transmissions of the same packet, but changes independently from packet to packet as in [11]. The independence assumption between channel responses from packet to packet may not be justified in practice, but it is adopted in this paper in order to evaluate the average system performance for all possible channel realizations from link to link. However, we keep the indexing of the channel response by the transmission index t for the sake of generality of the receiver structure. Moreover, we assume that the length of the cyclic prefix P is larger than the maximum delay spread $L_{\max}$. According to this model, the received sequence samples, denoted by $y^{(t)}(n)$, are given by

$$y^{(t)}(n) = \sum_{i=0}^{L-1} h^{(t)}(i) x^{(t)}(n-i) + w^{(t)}(n), \tag{2}$$

where $w^{(t)}(n)$ is an additive complex white Gaussian noise with variance σ_w^2 ($\sigma_w^2/2$ per real dimension).

We compare the achievable performance between the different transmission schemes under investigation assuming an optimal joint ML receiver with perfect channel state information at the receiver while no CSIT is assumed. A comparative analysis based on the average pairwise error probability (PEP) is presented in Section 3.

3. Error Probability Analysis

In order to compare the theoretical performance of the BID and the CFSD schemes, we consider an optimal ML receiver, and we compare the properties of the Euclidean distance distribution at the output of the frequency-selective channel for multiple transmissions.

Let $\mathbf{c}$ and $\hat{\mathbf{c}}$ be the transmitted and the estimated binary codewords after T transmissions. Let $\mathbf{x}_T = (\mathbf{x}^{(1)}, \ldots, \mathbf{x}^{(T)})$ and $\hat{\mathbf{x}}_T = (\hat{\mathbf{x}}^{(1)}, \ldots, \hat{\mathbf{x}}^{(T)})$ be the corresponding transmitted sequences. We define the error sequence between $\hat{\mathbf{x}}_T$ and $\mathbf{x}_T$ by $\mathbf{e}_T \triangleq (\mathbf{e}^{(1)}, \ldots, \mathbf{e}^{(T)}) = \hat{\mathbf{x}}_T - \mathbf{x}_T$. For a joint ML receiver, Forney has shown in [12] that the PEP between any pair of sequences is given as a function of the error sequence $\mathbf{e}_T$ between them by

$$P_2(\hat{\mathbf{c}}, \mathbf{c}) = Q\left(\sqrt{\frac{d_E^2(\mathbf{e}_T)}{4\sigma_w^2}}\right), \tag{3}$$

where $Q(\cdot)$ is the complementary distribution function of standard Gaussian, and d_E is the Euclidean distance between $\hat{\mathbf{x}}_T$ and $\mathbf{x}_T$ at the output of the noiseless channel. For a given set of channel realizations $\{\mathbf{h}^{(1)}, \ldots, \mathbf{h}^{(T)}\}$, the squared Euclidean distance d_E^2 can be evaluated as

$$d_E^2(\mathbf{e}_T) = \sum_{t=1}^{T} \sum_{n=0}^{N-1} \left| \sum_{i=0}^{L-1} h^{(t)}(i) e^{(t)}(n-i) \right|^2. \tag{4}$$

By developing the squared sum in (4) and performing some algebraic computations, we obtain

$$d_E^2(\mathbf{e}_T) = \sum_{t=1}^{T} \sum_{\ell=-L+1}^{L-1} R_\ell^\star\left(\mathbf{h}^{(t)}\right) R_\ell\left(\mathbf{e}^{(t)}\right), \tag{5}$$

where the superscript $(\cdot)^\star$ denotes the complex conjugate and $R_\ell(\cdot)$ is the deterministic periodic autocorrelation function for a lag ℓ, defined for an arbitrary complex sequence $\mathbf{x}$ of length N by $R_\ell(\mathbf{x}) \triangleq \sum_{n=0}^{N-1} x(n)x^\star(n-\ell)$ with $x(-n) = x(N-n)$. Expression (5) for the squared Euclidean distance is equivalent to that given by Forney in [12] using polynomial notations.

From (5), we note that the channel and the error sequence have a symmetrical effect on the Euclidean distance through their respective autocorrelation functions. By analogy to channel diversity, transmit diversity is a way to decrease the probability of error sequences leading to a low output Euclidean distance. In fact, the auto-correlation function of the error sequence $R_\ell(\mathbf{e}^{(t)})$ depends simultaneously on the Hamming weight of the binary error sequence, the interleaving, and the mapping scheme. Therefore, most of diversity techniques try to enhance the statistical distribution of d_E by modifying some system parameters such as the mapping [13], or by adding additional devices at the transmitter such as a binary precoder [8], for example.

For convenience, we denote the squared Euclidean distance by the new variable $\Delta_T \triangleq d_E^2(\mathbf{e}_T)$. We can rewrite (5) as the sum of two variables as follows:

$$\Delta_T = \Gamma_T + \Theta_T, \tag{6}$$

with

$$\Gamma_T \triangleq \sum_{t=1}^{T} R_0\left(\mathbf{h}^{(t)}\right) R_0\left(\mathbf{e}^{(t)}\right), \tag{7}$$

$$\Theta_T \triangleq 2\Re\left[\sum_{t=1}^{T} \sum_{\ell=1}^{L-1} R_\ell^\star\left(\mathbf{h}^{(t)}\right) R_\ell\left(\mathbf{e}^{(t)}\right)\right], \tag{8}$$

where $\Re[\cdot]$ denotes the real part. In (6), the first variable Γ_T takes positive real values reflecting the effect of the channel gain on the squared Euclidean distance, whereas the second variable Θ_T takes signed real values reflecting the fluctuation of the Euclidean distance due to the presence of the ISI. For an ISI-free channel, it is obvious that $\Theta_T = 0$ and the performance limit for channel equalization are only determined by the properties of Γ_T.

The PEP depends actually on the Hamming weight d of the binary error codeword between $\hat{\mathbf{c}}$ and $\mathbf{c}$. The average PEP over the space of all possible error sequences of a given Hamming weight d and all channel realizations depends on the statistical distribution of Δ_T over this probability space. Since its difficult in general to analytically derive the probability density function (pdf) of Δ_T, we compare different transmission schemes by comparing the main statistical properties of Δ_T for each scheme, that is, the mean and the variance. A higher mean value and/or a smaller variance indicates better error performance. First, we compare the limiting performance of both diversity schemes assuming perfect interference cancellation by the receiver, then we compare the ISI power between them.

3.1. Performance Limits. A lower bound on the PEP can be obtained by assuming that the ISI is completely removed by the receiver, that is, $\Theta_T = 0$ and $\Delta_T = \Gamma_T$. This is equivalent to packet transmission over an equivalent flat-fading channel with an equivalent squared gain of $\gamma^{(t)} = R_0(\mathbf{h}^{(t)}) = \|\mathbf{h}^{(t)}\|^2$. This bound is usually referred to as the matched filter lower bound (MFB). Assuming that the channel remains the same for all retransmissions $\mathbf{h}^{(t)} = \mathbf{h}$ and defining $\varepsilon^{(t)} = \|\mathbf{e}^{(t)}\|^2$, we can rewrite (7) as

$$\Gamma_T = \gamma \sum_{t=1}^{T} \varepsilon^{(t)}. \tag{9}$$

The variable $\varepsilon^{(t)}$ depends on the binary error pattern and the underlying modulation. For each diversity scheme, we will calculate the mean and the variance of Γ_T.

For the CFSD scheme, multiplying each symbol by a unit amplitude complex number does not change the amplitude of the error symbol. Therefore, the variables $\varepsilon^{(t)}$ are identical. Let μ_e and σ_e^2 be the mean and the variance of $\varepsilon^{(1)}$. Let μ_h and σ_h^2 be the mean and the variance of the squared channel gain γ. Using the independence between $\varepsilon^{(1)}$ and γ, we obtain the following expressions for the mean and the variance of Γ_T:

$$\mu_{\mathrm{CFSD}}(\Gamma_T) = T\mu_h\mu_e, \tag{10}$$

$$\sigma^2_{\mathrm{CFSD}}(\Gamma_T) = T^2\mu_e^2\sigma_h^2 + T^2\left(\mu_h^2 + \sigma_h^2\right)\sigma_e^2. \tag{11}$$

Consequently, the performance limits for the CFSD scheme are the same as for the IT scheme.

For the BID scheme, assuming independent interleavers, the variables $\varepsilon^{(t)}$ are i.i.d. random variables. In this case we obtain

$$\mu_{\mathrm{BID}}(\Gamma_T) = T\mu_h\mu_e, \tag{12}$$

$$\sigma^2_{\mathrm{BID}}(\Gamma_T) = T^2\mu_e^2\sigma_h^2 + T\left(\mu_h^2 + \sigma_h^2\right)\sigma_e^2. \tag{13}$$

For a given mapping scheme the computation of μ_e and σ_e^2 is shown in the appendix under the uniform interleaving assumption [14] which gives the average estimations over all possible deterministic random interleavers. Note that μ_e and σ_e depend on the Hamming weight d.

By comparing (11) with (13), we note that the second term in the variance expression for the CFSD scheme is reduced by a factor T for the BID scheme. This reflects the inherent modulation diversity of the BID scheme because error bits are located in different symbols at each retransmission. However, in some special cases such as BPSK and QPSK modulations with Gray mapping, $\varepsilon^{(t)}$ is invariant to bit-interleaving. Indeed, we have $\varepsilon^{(t)} = \alpha d$, where $\alpha = 4$ for BPSK and $\alpha = 2$ for QPSK. Consequently, we have $\sigma_e^2 = 0$, and both diversity schemes have the same performance limits as for the IT scheme in this case. By contrast, for a higher order modulation such as 16-QAM or 64-QAM, $\sigma_e^2 \neq 0$ and some variance reduction can be expected.

3.2. Intersymbol Interference Power. In this section, we show the effect of both diversity schemes on the interference power by evaluating the variance of the variable Θ_T. For the long-term static channel model, (8) can be written as

$$\Theta_T = 2\Re\left[\sum_{\ell=1}^{L-1} R_\ell^\star(\mathbf{h}) S_\ell\right], \tag{14}$$

where $S_\ell = \sum_{t=1}^{T} R_\ell(\mathbf{e}^{(t)})$. Assuming that the channel tap coefficients are independent with zero mean, this implies that $R_\ell^\star(\mathbf{h})$ are zero mean random variables and pairwise uncorrelated for different ℓ. Consequently, Θ_T is also a zero mean random variable. In addition, we assume that both the channel response and the error sequence have the same power per real dimension; the variance of Θ_T can be computed as

$$\sigma^2(\Theta_T) = \mathbb{E}\left(|\Theta_T|^2\right) = 2\sum_{\ell=1}^{L-1} \mathbb{E}\left(\left|R_\ell^\star(\mathbf{h})\right|^2\right)\mathbb{E}\left(|S_\ell|^2\right). \tag{15}$$

The difference between both transmit diversity schemes concerns the value of $\mathbb{E}(|S_\ell|^2)$. Thanks to the interleaver, we can assume that error symbols e_n in the transmitted packet are uncorrelated (but not independent due to the constraint on their total Hamming weight d). Consequently, the random variables $R_\ell(\mathbf{e}^{(t)})$ have a zero mean and pairwise uncorrelated for different ℓ. This yields

$$\mathbb{E}\left(|S_\ell|^2\right) = \sum_{t=1}^{T} \mathbb{E}\left(\left|R_\ell\left(\mathbf{e}^{(t)}\right)\right|^2\right). \tag{16}$$

Moreover, two error symbols e_i and e_j are conditionally independent to their respective Hamming weight k_i and k_j. Using all previous assumptions, it is straightforward to compute the variance of S_ℓ for both diversity schemes.

For the BID scheme we obtain

$$\mathbb{E}\left(|S_\ell|^2\right)_{\text{BID}} = \overline{\rho}_s(N-\ell)T, \tag{17}$$

where $\overline{\rho}_s = \mathbb{E}(|s_i|^2|s_j|^2)$ for $i \neq j$ which can be computed as indicated in the appendix.

For the CFSD scheme we obtain

$$\mathbb{E}\left(|S_\ell|^2\right)_{\text{CFSD}} = \overline{\rho}_s(N-\ell)\lambda_\ell, \tag{18}$$

where

$$\lambda_\ell = \left|\sum_{t=1}^{T} e^{-j2\pi\ell\nu^{(t)}}\right|^2. \tag{19}$$

We remark from (15) that the variance $\sigma^2(\Theta_T)$ depends on the power-delay profile of the channel. Since no CSIT is assumed, the optimal frequency-shift values are those that minimize the objective function $J_T = \sum_{\ell=1}^{L-1} \lambda_\ell^2$. As it is shown in [15], this function can achieve its absolute minimum value when

$$\lambda_\ell = T\frac{L-T}{L-1}, \quad \forall \ell, T < L. \tag{20}$$

This minimum value could be achieved by a proper choice of $\nu^{(t)}$ from the set $\{k/L : k = 0, \ldots, L-1\}$. For unknown channel length L, frequency shifts can be chosen as the maximum possible in order to take account for the shortest channel memory.

By comparing the value of $\mathbb{E}(|S_\ell|^2)$ for the BID scheme given in (17) with its value for the CFSD scheme given in (18), we note that the CFSD scheme leads to a smaller interference variance $\sigma^2(\Theta_T)$ because $\lambda_\ell < T$. In the particular case when $T = L$, we can have $\lambda_\ell = 0$, hence $\sigma^2(\Theta_T) = 0$ which means that the interference is completely cancelled by the CFSD scheme.

For large values of channel memory L, we have $\lambda_\ell \approx T$ and the difference between the two diversity schemes with regard to the ISI power becomes smaller. Note that for the IT scheme, we have $\mathbb{E}(|S_\ell|^2) = \rho_s(N-\ell)T^2$ which is obtained by setting $\nu^{(t)} = 0$ in (18).

In conclusion, the BID scheme has a better performance limit than the CFSD scheme for high-order modulations, but the CFSD scheme is more efficient in combating the interference for a short channel memory.

4. Iterative Receiver Structure

It is known that the performance of an optimal ML receiver can be approached by using an iterative equalization and decoding approach as in turboequalization. In this section we present the structure of the turboequalizer with integrated packet combining for both diversity schemes with the purpose of showing the performance-complexity tradeoff achieved by these diversity techniques.

4.1. Cyclic Frequency-Shift Diversity. The receiver structure for the CFSD scheme is shown in Figure 2. For each received frame $\mathbf{y}^{(t)}$, the CP is first removed and then a discrete Fourier transform (DFT) is applied in order to perform equalization in the frequency domain. In the following, the DFTs of signals are denoted by capital letters as a function of the normalized frequency ν. Thanks to the cyclic prefix insertion, the time-domain convolution becomes a simple multiplication in the frequency domain. The received frame can be written as

$$Y^{(t)}(\nu) = H^{(t)}(\nu)X^{(t)}(\nu) + W^{(t)}(\nu). \tag{21}$$

The inverse frequency shift is performed on $Y^{(t)}$ to obtain $Z^{(t)}$ which is given by

$$\begin{aligned} Z^{(t)}(\nu) &= Y^{(t)}(\nu - \nu_t) \\ &= H^{(t)}(\nu - \nu_t)S(\nu) + W^{(t)}(\nu - \nu_t) \\ &= \widetilde{H}^{(t)}(\nu)S(\nu) + \widetilde{W}^{(t)}(\nu). \end{aligned} \tag{22}$$

This gives the equivalent single-input multiple-output (SIMO) model for the CFSD scheme, where $\widetilde{H}^{(t)}$ is the equivalent channel and $\widetilde{W}^{(t)}$ is the equivalent noise. The signals $Z^{(t)}$ are then processed by a turboequalizer including two soft-input soft-output (SISO) modules which are connected

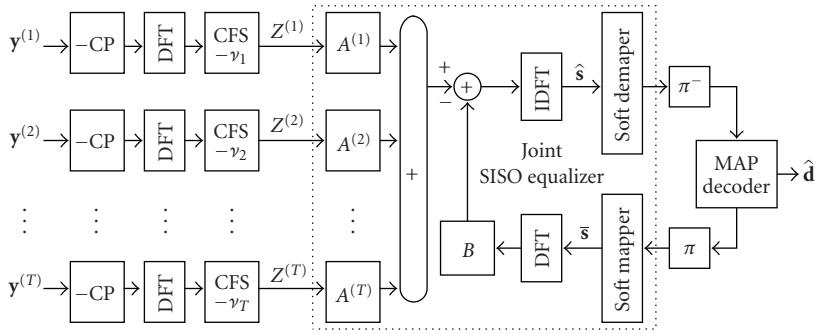

Figure 2: Iterative receiver structure for the CFSD scheme with joint equalization.

iteratively through the interleaver. One SISO module for joint MMSE equalization operating in the frequency domain and another SISO module for a maximum a posteriori (MAP) channel decoding [16] operating in the time domain. The joint MMSE equalizer includes multiple forward linear filters $A^{(t)}$ and a backward filter B. According to this structure, the linear estimate $\hat{\mathbf{s}}$ of $\mathbf{s}$ after T transmissions is given by

$$\hat{S} = \sum_{t=1}^{T} A^{(t)} Z^{(t)} - B\bar{S}. \tag{23}$$

Following the same analysis in [17, 18] and using the equivalent SIMO model, the derivation of the MMSE filters that minimize the mean square error $E[|\hat{s}(n) - s(n)|^2]$ is straightforward and leads to the following solution:

$$\begin{aligned} A^{(t)} &= \frac{\left(\widetilde{H}^{(t)}\right)^*}{\sigma_w^2 + \nu \sum_{t=1}^{T} \left|\widetilde{H}^{(t)}\right|^2}, \\ B &= \sum_{t=1}^{T} A^{(t)} \widetilde{H}^{(t)} - \mu, \\ \nu &= \frac{1}{N} \sum_{n=0}^{N-1} \mathrm{var}(\bar{s}(n)), \\ \mu &= \frac{1}{N} \sum_{k=0}^{N-1} \frac{H_T^2(k/N)}{\sigma_w^2 + \nu H_T^2(k/N)}, \end{aligned} \tag{24}$$

where H_T is the compound channel defined by its squared amplitude $H_T^2 \triangleq \sum_{t=1}^{T} |\widetilde{H}^{(t)}|^2$ and ν is reliability of the decoder feedback, where $\nu = 0$ indicates a perfect feedback, and $\nu = 1$ for no a priori. The output of the MMSE estimator can be written in the time domain after an IDFT using the Gaussian model for the estimated symbols as

$$\hat{s}(n) = \mu s(n) + \eta(n), \tag{25}$$

where η is a complex Gaussian noise with zero mean and variance $\sigma_\eta^2 = \mu(1 - \nu\mu)$. The output extrinsic a posteriori probabilities (APPs) are given by

$$\mathrm{APP}(s(n) = s \in \mathcal{S}) = K \exp\left(-\frac{|\hat{s}(n) - \mu s|^2}{\sigma_\eta^2}\right), \tag{26}$$

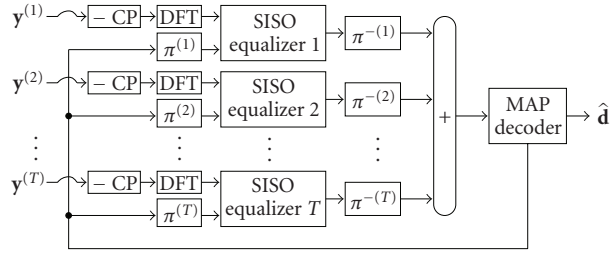

Figure 3: Iterative receiver structure for the BID scheme with separate equalization and LLR combining.

where K is a normalization factor in order to have a true probability mass function. The extrinsic log-likelihood ratios (LLRs) of the coded bits are then computed by soft demapping in order to decode the received frame by a MAP decoder after deinterleaving. For an iterative processing, the decoder's soft decisions in the form of extrinsic LLRs are interleaved and returned to the equalizer which, in turn, produces soft symbol decisions $\bar{\mathbf{s}}$ to be used as priory in the next iteration. Note that for separate detection and decoding, one can put the equalizer's soft input to zero ($\nu = 1$).

With regard to the system complexity, we see that the CFSD requires only N additional complex multiplications at the transmitter and a simple vector shift operation at the receiver. In addition, the complexity of the joint MMSE equalizer in the frequency domain is almost the same as for an MMSE equalizer with a single input. To show that, we note that the numerator of each forward filter is the matched filter to the channel which does not change with turboiterations. Hence, it is performed once per transmission. Since the denominator is common for all forward filters, the division can be performed after summation of the matched filters outputs. Consequently, for each new reception, the accumulated sum of the matched filters is updated and the same for the squared compound channel. Other operations are the same as for an equalizer with single input.

4.2. Bit-Interleaving Diversity. Joint equalization for the BID scheme is not possible because the transmitted symbols at each HARQ round are different. Therefore, we perform a

Table 1: Simulation parameters.

Parameter	Value
Frame length	$N = 516$ for QPSK, $N = 258$ for 16-QAM
Symbol rate	7.68 Msps
CP length	$P = 64$
Channel model	SCME urban macroscenario
Shaping filter	Raised cosine with roll off 0.23
Doppler	No Doppler

postcombining at the bit level by adding the LLRs issued from all equalizers as shown in Figure 3. The structure of the SISO equalizer is similar to the joint equalizer presented for the CFSD scheme with only one single input.

Here, we need for each turboiteration two DFT operations and two interleaving operations per equalizer. Since there is T parallel equalizers in the BID scheme, the complexity of the receiver increases linearly with the number of transmissions. While in the CFSD scheme, there is one joint equalizer which requires only two DFTs and two interleaving operations per turbo-iteration independently of the number of transmissions. Therefore, the BID scheme has a larger complexity in comparison with the CFSD scheme if turbo-equalization is performed.

5. Results

In this section, we present some simulation results comparing the performance of the two transmit diversity schemes for different system configurations.

Simulations are performed using the 3GPP Spatial Channel Model Extended (SCME) of the European WINNER framework as specified in [19, 20] in the case of monoantenna transmission. This channel model is characterized by six nonzero taps with varying delays per link. For each transmitted packet, a random channel realization is generated and then used for all HARQ retransmissions of the packet. The system performance is evaluated in terms of FER versus the average SNR defined by $E_s/N_0 = 1/\sigma_w^2$. We assume that the maximum of HARQ transmissions is $T_{\max} = 4$. For the CFSD scheme, frequency-shift parameters are $\nu^{(1)} = 0$, $\nu^{(2)} = 1/2$, $\nu^{(3)} = 1/4$, and $\nu^{(4)} = 3/4$. All used interleavers are pseudorandom interleavers. Other simulation parameters inspired from the LTE standard [21] are listed in Table 1. Monte Carlo simulations are performed over a maximum of 5000 packets.

We first consider a noncoded transmission system in order to show the intrinsic gain for both diversity schemes compared to the identical transmission scheme. This corresponds to the system performance before channel decoding for coded systems. Figure 4 shows the FER performance versus the average SNR after the last HARQ round ($T = 4$) for QPSK and 16-QAM modulations.

We can observe the superiority of the CFSD scheme among all transmission schemes due to its best capability in interference mitigation. For QPSK modulation, we have SNR gain at FER = 10^{-2} of about 2 dB for the BID scheme and

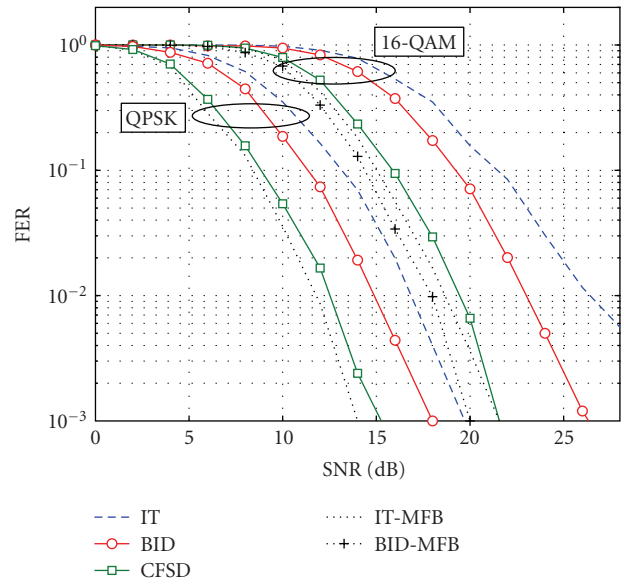

Figure 4: FER performance comparison between different transmission schemes for a non coded system using QPSK and 16-QAM modulations.

4 dB for the CFSD scheme in comparison with the IT scheme. Note that the CFSD scheme is only at 0.4 dB of the MFB which is the same for all schemes. For 16-QAM modulation, the MFB for the BID scheme gives the best performance, but the better performance for the CFSD scheme is due to better performance of the joint equalization compared to the LLR combining used for the BID scheme. It is true that the used channel has a large channel memory which may attain more than 100 symbol periods, but it has a decreasing power-delay profile with most of the interference power originating from the less delayed paths. In this sense, the effective channel memory is not very large. This explains the larger interference reduction in the case of the CFSD scheme.

Now, we consider a coded system with a noniterative receiver including separate equalization and channel decoding without turboiteration. The performance of the noniterative receiver is obtained by performing one equalization step followed by one channel decoding step.

The channel code is the LTE turbocode of rate-1/3 using two identical constituent convolutional codes $(1, 15/13)_8$ with quadratic permutation polynomial internal interleaver of length $K = 344$ taken from [21, (Table 5.1.3-3)]. For simplicity, no trellis termination is performed for the component codes. The receiver performs one equalization step followed by one channel decoding step. The channel decoder itself performs a maximum of five internal iterations between the two internal convolutional decoders in the turbodecoder. Simulation results are given in Figure 5 for both QPSK and 16-QAM modulations. Using a powerful code, both diversity schemes have almost similar performances. We can observe that the performance of the BID scheme is still far from the corresponding MFB for 16-QAM modulation. Note that for high throughput requirements, bit-puncturing can be applied in order to increase the coding rate. For a higher

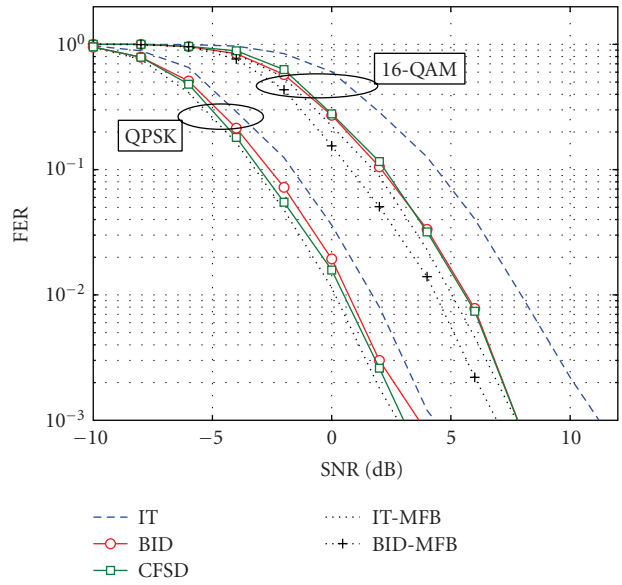

Figure 5: FER performance comparison between different transmission schemes for a coded system using a turbo-code for QPSK and 16-QAM modulations.

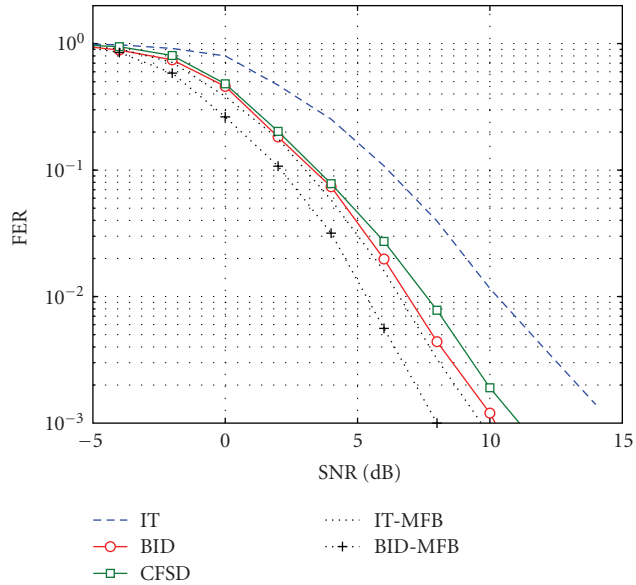

Figure 6: FER performance for different transmission schemes for a coded system with a rate-1/3 convolutional code using 16-QAM modulation and linear detection.

coding rate, the performance gains of the proposed diversity schemes lay somewhere between the full rate case (rate 1/3) and the uncoded case. In order to close this gap, an iterative processing can be performed between the detector and the channel decoder. Due to the high complexity of the iterative processing using a turbocode, we use the LTE convolutional code of rate-1/3 whose generator polynomial is $(133, 171, 165)_8$. Here again, no trellis termination is performed for convolutional codes. Figure 6 shows the FER performance at the last HARQ round for separate detection and decoding, while Figure 7 shows the corresponding FER performance for a turbo-equalizer which performs a maximum of four turbo-iterations.

We note that for a linear receiver without turbo-iterations, the performance of both diversity schemes is almost the same. With a turbo-equalizer, the BID scheme outperforms the CFSD scheme unlike the noncoded system because the iterative receiver performs closely to the MFB which is better for the BID scheme.

In conclusion, we find that the CFSD is suitable for a linear receiver with separate equalization and decoding, especially for high rate channel coding. The BID scheme gives better performance with an iterative receiver at the expense of a higher system complexity.

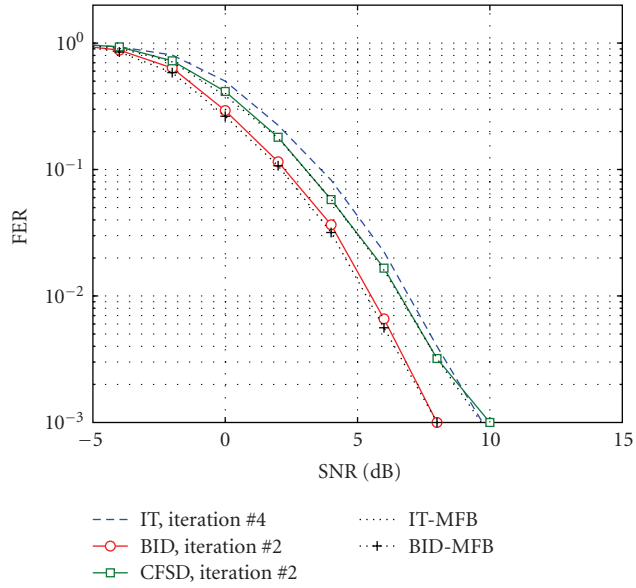

Figure 7: FER performance for different transmission schemes for a coded system with a rate-1/3 convolutional code using 16-QAM modulation and turbo-equalization.

6. Conclusions

We have presented and compared two transmit diversity schemes for multiple HARQ retransmission using single carrier signaling over frequency selective channels. Our theoretical analysis shows that the BID scheme has better performance limits than the CFSD scheme for high order modulation, but the CFSD scheme is more efficient in combating the ISI for channels with short memory. The CFSD is suitable for a linear receiver with separate equalization and decoding, while the BID scheme gives a better performance with an iterative receiver at the expense of a higher system complexity. These diversity schemes can be used in order to compensate for poor channel diversity in slow fading environment depending to the desired performance complexity tradeoff and the system parameters including the channel coding rate, the modulation order.

Appendix

Assuming uniform interleaving, the error symbols are considered as identically distributed but not independent due the constraint on the sum of their Hamming weights. However, any two error symbols are conditionally independent knowing their respective Hamming weights. The coded and interleaved packet contains NQ bits which are modulated to N symbols. The error packet contains d errors which are assumed uniformly distributed over the packet. The probability that a symbol e_n has a Hamming weight $d_H(e_n) = k$ is given by

$$\Pr(d_H(e_n) = k) = \frac{\binom{Q}{k}\binom{NQ-Q}{d-k}}{\binom{NQ}{d}}. \tag{A.1}$$

The average squared amplitude μ_e can be calculated as

$$\begin{aligned}\mu_e(d) &= \mathbb{E}\left[\|\mathbf{e}\|^2 \mid d\right] \\ &= N\sum_{k=1}^{Q} m_2(k)\Pr(d_H(e_n) = k) \\ &= N\binom{NQ}{d}^{-1}\sum_{k=1}^{Q}\binom{Q}{k}\binom{NQ-Q}{d-k}m_2(k),\end{aligned} \tag{A.2}$$

where $m_2(k) = \mathbb{E}[|e_n|^2 \mid k]$ for $k = 1, \ldots, Q$ is the conditional mean of $|e_n|^2$ giving its Hamming weight k.

The variance σ_e^2 can be similarly calculated as follows:

$$\sigma_e^2(d) = \mathbb{E}\left[\left(\|\mathbf{e}\|^2 - \mu_e\right)^2 \mid d\right] = \mathbb{E}\left[\|\mathbf{e}\|^4 \mid d\right] - \mu_e^2(d), \tag{A.3}$$

where

$$\begin{aligned}\mathbb{E}\left[\|\mathbf{e}\|^4 \mid d\right] &= N\overline{m}_4(d) + N(N-1)\overline{\rho}_2(d), \\ \overline{m}_4(d) &= \mathbb{E}\left[|e_n|^4 \mid d\right] \\ &= \binom{NQ}{d}^{-1}\sum_{k=1}^{Q}\binom{Q}{k}\binom{NQ-Q}{d-k}m_4(k), \\ \overline{\rho}_2(d) &= \mathbb{E}\left[|e_{n_1}|^2|e_{n_2}|^2 \mid d\right] \\ &= \binom{NQ}{d}^{-1} \\ &\quad\times\sum_{\substack{k_1,k_2=1 \\ k_1+k_2\le d}}^{Q}\binom{Q}{k_1}\binom{Q}{k_2}\binom{NQ-2Q}{d-k_1-k_2}m_2(k_1)m_2(k_2),\end{aligned} \tag{A.4}$$

for $n_1 \neq n_2$, where $m_4(k) = \mathbb{E}[|e_n|^4 \mid k]$. The conditional moments m_2 and m_4 can be computed directly from the modulation and the mapping scheme.

Acknowledgment

This work was supported by the project "Urbanisme des Radiocommunications" of the Pôle de compétitivité SYSTEM@TIC.

References

[1] 3GPP Technical Specification Group Radio Access Network E-UTRA (Release 8), "LTE physical layer-general description," 3GPP TS 36.201 V8.3.0, March 2009, http://www.3gpp.org/ftp/Specs/html-info/36-series.htm.

[2] S. Lin, D. Costello Jr., and M. Miller, "Automatic-repeat-request error-control schemes," *IEEE Communications Magazine*, vol. 22, no. 12, pp. 5–17, 1984.

[3] C. Douillard, A. Picart, P. Didier, M. Jézéquel, C. Berrou, and A. Glavieux, "Iterative correction of intersymbol interference: turbo-equalization," *European Transactions on Telecommunications and Related Technologies*, vol. 6, no. 5, pp. 507–512, 1995.

[4] H. Harashima and H. Miyakawa, "Matched-transmission technique for channels with intersymbol interference," *IEEE Transactions on Communications*, vol. 20, no. 4, pp. 774–780, 1972.

[5] G. D. Forney Jr. and M. V. Eyuboglu, "Combined equalization and coding using precoding," *IEEE Communications Magazine*, vol. 29, no. 12, pp. 25–34, 1991.

[6] H. Samra, H. Sun, and Z. Ding, "Capacity and linear precoding for packet retransmissions," in *Proceedings of the IEEE International Conference on Acoustics, Speech, and Signal Processing (ICASSP '05)*, vol. 3, pp. 541–544, 2005.

[7] A.-N. Assimi, C. Poulliat, I. Fijalkow, and D. Declercq, "Periodic Hadamard phase precoding for HARQ systems over intersymbol interference channels," in *Proceedings of the IEEE International Symposium on Spread Spectrum Techniques and Applications (ISSSTA '08)*, pp. 714–718, Bologna, Italy, 2008.

[8] D. N. Doan and K. R. Narayanan, "Iterative packet combining schemes for intersymbol interference channels," *IEEE Transactions on Communications*, vol. 50, no. 4, pp. 560–570, 2002.

[9] A.-N. Assimi, C. Poulliat, and I. Fijalkow, "Packet combining for turbo-diversity in HARQ systems with integrated turbo-equalization," in *Proceedings of the 5th International Symposium on Turbo Codes and Related Topics (TURBOCODING '08)*, pp. 61–66, Lausanne, Switzerland, 2008.

[10] H. Samra and Z. Ding, "Symbol mapping diversity in iterative decoding/demodulation of ARQ systems," in *Proceedings of IEEE International Conference on Communications (ICC '03)*, vol. 5, pp. 3585–3589, Anchorage, Alaska, USA, 2003.

[11] H. El Gamal, G. Caire, and M. O. Damen, "The MIMO ARQ channel: diversity-multiplexing-delay tradeoff," *IEEE Transactions on Information Theory*, vol. 52, no. 8, pp. 3601–3621, 2006.

[12] G. D. Forney Jr., "Maximum-likelihood sequence estimation of digital sequences in the presence of intersymbol interference," *IEEE Transactions on Information Theory*, vol. 18, no. 3, pp. 363–378, 1972.

[13] H. Samra, Z. Ding, and P. M. Hahn, "Optimal symbol mapping diversity for multiple packet transmissions," in *Proceedings of the IEEE International Conference on Acoustics, Speech, and Signal Processing (ICASSP '03)*, vol. 4, pp. 181–184, Hong Kong, 2003.

[14] S. Benedetto, D. Divsalar, G. Montorsi, and F. Pollara, "Serial concatenation of interleaved codes: performance analysis,

design, and iterative decoding," *IEEE Transactions on Information Theory*, vol. 44, no. 3, pp. 909–926, 1998.

[15] P. Xia, S. Zhou, and G. B. Giannakis, "Achieving the Welch bound with difference sets," *IEEE Transactions on Information Theory*, vol. 51, no. 5, pp. 1900–1907, 2005.

[16] L. Bahl, J. Cocke, F. Jelinek, and J. Raviv, "Optimal decoding of linear codes for minimizing symbol error rate," *IEEE Transactions on Information Theory*, vol. 20, no. 2, pp. 284–287, 1974.

[17] R. Visoz, A. O. Berthet, and S. Chtourou, "Frequency-domain block turbo-equalization for single-carrier transmission over MIMO broadband wireless channel," *IEEE Transactions on Communications*, vol. 54, no. 12, pp. 2144–2149, 2006.

[18] T. Ait-Idir, H. Chafnaji, and S. Saoudi, "Joint hybrid ARQ and iterative space-time equalization for coded transmission over the MIMO-ISI channel," in *Proceedings of the IEEE Wireless Communications and Networking Conference (WCNC '08)*, pp. 622–627, Las Vegas, Nev, USA, March 2008.

[19] D. S. Baum, J. Hansen, and J. Salo, "An interim channel model for beyond-3G systems: extending the 3GPP spatial channel model (SCM)," in *Proceedings of the IEEE Vehicular Technology Conference (VTC '05)*, vol. 5, pp. 3132–3136, Zurich, Switzerland, 2005.

[20] J. Salo, et al., "Matlab implementation of the 3GPP spatial channel model (3GPP TR 25.996)," 2005, http://www.ist-winner.org/3gpp_scm.html.

[21] 3GPP Technical Specification Group Radio Access Network E-UTRA (Release 8), "Base station (BS) radio transmission and reception," 3GPP TS 36.104 V8.5.0, March 2009, http://www.3gpp.org/ftp/Specs/html-info/36-series.htm.